Journal of Thermal Analysis and Calorimetry (2023) 148:10557–10572
https://doi.org/10.1007/s10973-023-12258-2

# Thermal characterization of acrylonitrile butadiene styrene-ABS obtained with different manufacturing processes

**Alain Alonso[1] · Mariano Lázaro[1] · David Lázaro[1] · Daniel Alvear[2]**

Received: 29 October 2022 / Accepted: 6 May 2023 / Published online: 24 May 2023


## Abstract

Polymers are widely employed in many areas, e.g. transport, packaging, electronic devices, etcetera. Among them, acrylonitrile–butadiene–styrene (ABS) is one of the most employed polymers due to its mechanical properties, its ease to mechanize and recyclability. Nevertheless, according to the fire properties, ABS behaviour is usually worse than other polymers, therefore, they have to be upgraded with flame retardant additives. To characterize the fire behaviour of a certain material is necessary to address several typology of tests, providing relevant properties such as thermal conductivity, flammability and heat released. However, researchers may not always be able to run all tests due to the lack of apparatus or samples. Therefore, it is necessary to seek bibliographic sources. As one might expect, for a given material, the property values should be similar, regardless of who performs the test. However, sometimes slightly different results are obtained, which may be due to different causes, such as differences in test set-up and in material composition/manufacture. These differences in properties may lead researcher to doubt which data to use. This paper presents the results of different types of tests using neat ABS polymer. Additionally, these results are compared with the data from literature, discussing the similarities/differences and offering a more comprehensive characterization of ABS. The laboratory techniques included in this work are: thermogravimetric analysis, differential scanning calorimetry, laser flash analysis, smoke density, cone calorimeter, fire propagation and flammability.

**Keywords** ABS · Polymer · Thermal properties · Flame spread · Heat release rate · Flammability

**Abbreviations**

| | |
|---|---|
| ABS | Acrylonitrile–butadiene–styrene |
| $C_2H_4$ | Ethylene |
| $C_2H_6$ | Ethane |
| $C_3H_4O$ | Acrolein |
| $C_3H_8$ | Propane |
| $C_6H_{14}$ | Hexane |
| $C_6H_6O$ | Phenol |
| $CH_2O$ | Formaldehyde |
| $CH_4$ | Methane |
| CO | Carbon monoxide |
| $CO_2$ | Carbon dioxide |
| DSC | Differential scanning calorimetry |
| EHC | Effective heat of combustion/MJ $kg^{-1}$ |
| FIGRA | Fire growth parameter/kW/$m^{-2}$ $s^{-1}$ |
| FMVSS | Federal motor vehicle safety standard |
| FTIR | Fourier transform infrared spectroscopy |
| HBr | Hydrogen bromide |
| HCl | Hydrogen chloride |
| FMVSS | Federal motor vehicle safety standard |
| HCN | Hydrogen cyanide |
| HF | Hydrogen fluoride |
| HR | Heating rate/K $min^{-1}$ |
| HRR | Heat release rate/kW $m^{-2}$ |
| LFA | Laser flash analysis |
| LOI | Limited oxygen index |
| LLDPE | Linear low-density polyethylene |
| MLR | Mass-loss rate/% $°C^{-1}$ and g $s^{-1}$ |
| $N_2O$ | Nitrogen dioxide |
| $NH_3$ | Ammonia |
| NO | Nitrogen monoxide |
| $NO_2$ | Nitrous oxide |
| NOx | Nitrogen oxides |
| pMLR | Peak mass-loss rate/% $°C^{-1}$ and g $s^{-1}$ |
| PMMA | Poly(methyl methacrylate) |
| SEA | Specific smoke extinction area/$m^2$ $kg^{-1}$ |
| $SO_2$ | Sulphur dioxide |
| TG | Thermogravimetric analysis |

✉ Alain Alonso
alonsoia@unican.es

[1] GIDAI, Universidad de Cantabria, Avda. Los Castros, s/n, 39005 Santander, Spain

[2] General Directorate of Industry, Energy and Mines, Government of Cantabria, Cantabria, Spain

| | |
|---|---|
| TSP | Total smoke production/$m^2$ |
| UL | Underwriters laboratories |

**Letters**

| | |
|---|---|
| $B$ | Burn rate/mm $min^{-1}$ |
| $C_p$ | Specific heat/kJ $kg^{-1}$ $K^{-1}$ |
| $I$ | Thermal inertia/kJ $m^{-2}$ $K^{-1}$ $s^{-1/2}$ |
| $K$ | Extinction coef. visible smoke/1 $m^{-1}$ |
| $S_d$ | Smoke density (–) |

**Greek letters**

| | |
|---|---|
| $\propto$ | Diffusivity/$mm^2$ $s^{-1}$ |
| $k$ | Thermal conductivity/W $m^{-1}$ $K^{-1}$ |
| $\rho$ | Density/kg $m^{-3}$ |

## Introduction

Nowadays polymers, either natural or synthetic, are widely employed in several industries [1] such as packaging, electronic, transportation and construction. The massive employment of polymers could be explained due to their low cost and their inherent properties, e.g. lightweight, easy machining and durability.

The acrylonitrile–butadiene–styrene, well known as ABS, is extensively used for various industries, estimating its market size in 2016 at USD 23.09 billion [2]. The lightweight of ABS makes attractive its employment especially in automotive and transport industry, since its lightweight favours fuel economy. The ABS has low thermal stability and high flammability [3]; hence, it is crucial to analyse its fire properties such as ignition temperature, heat release rate and flame spread in order to guarantee a safety use.

Habitually, to analyse the fire behaviour and obtain the thermal properties of a material, it is required to carry out several typologies of tests, i.e. a comprehensive characterization involves an extensive testing campaign. These tests can be classified as follows: (i) structural analysis (e.g. scanning electron microscopy and X-ray diffraction); (ii) thermal stability (e.g. thermogravimetric analysis (TG), differential scanning calorimetry (DSC) and laser flash analysis (LFA)) and (iii) flammability (e.g. cone calorimetry, fire propagation apparatus and UL-94, limited oxygen index (LOI)).

Studies of ABS from literature, neat or blended with other additives, are focused mostly in one or in limited number properties or types of tests, e.g. flammability, diffusivity, heat capacity, etcetera, not including other tests. For instance: in [4] are employed 3 techniques: spectroscopic analysis, TG analysis and UL-94; in [5] uniquely the diffusivity is analysed; in [6] an analysis was carried out employing TG analysis, cone calorimeter, LOI and Fourier transform infrared spectroscopy (FTIR); in [7] are used only cone calorimeter and UL-94. Hence, if researchers require a set of properties in their investigation, they have to check this information from several sources. This task should not represent a handicap since the large number of publications concerning the ABS. However, we found discrepancies in results between publications, even those using the same material and experimental boundary conditions, as the authors found in [8] for the PMMA poly(methyl methacrylate) in thermogravimetric analysis and cone calorimeter tests.

It seems obvious, therefore, that in each test is unlikely to obtain same results as previous ones; nonetheless, this could be reasonable up to a certain degree of discrepancy. The differences observed, for some techniques, are large enough to assume that they arise from parameters such as initial sample mass, as it was observed in [9] for the PMMA and linear low-density polyethylene (LLDPE). For instance, in cone calorimeter tests, the unexposed face of the sample plays an important role due to its configuration modifies the amount of heat flux that leaves the sample through this face changing the results, as the authors observed in [10] for the electrical cables. This information on a characteristic that actually determines the behaviour of the material is not always available, causing uncertainty in the use of the data.

At this point, some questions arise about what data we should use to define the properties of ABS in the most precise way. Hence, this work aims to expose a general characterization and review of ABS fire properties, providing the relevant information about the set-up of the experiments, and explaining the divergences in the results. To cope with the objective, we carried out an extensive campaign of tests, providing all information available about the sample and set-up, and collecting and comparing results from the other studies of different ABS available in literature.

The data presented in this paper intends to represent a baseline and reference of neat ABS polymer. In this way, any forthcoming study that intends to modify any property and parameter of ABS could use this work as a reference.

## Material and methods

In this work, the analysed polymer was neat ABS P2MC [11] manufactured by ELIX ®, i.e. this polymer did not include any type of blend or fire retardant. Its density at 23 °C was 1030 g $cm^{-3}$. The acrylonitrile–butadiene–styrene (ABS) is grafted thermoplastic polymer made of acrylonitrile (A), styrene (S) and polybutadiene (PB).

Habitually, to characterize the fire hazard of a certain material, it is necessary to be aware of properties related mainly with the flammability [12] such as: (i) ignition temperature, (ii) combustion, (iii) heat release rate and total heat released, (iv) flame spread, (v) propagation, (vi) smoke density and (vii) the toxicity of released gases. In addition, it is also required to

understand the thermal stability and the thermal decomposition processes [13].

The techniques employed to fulfil the aim of this paper are: simultaneous thermal analysis (STA) [14] [15]; laser flash analysis (LFA) [16]; smoke density test [17]; cone calorimetry [18]; horizontal propagation [19]; flammability [20] and limited oxygen index (LOI) [21]. These techniques and how tests were carried out are detailed below.

## Simultaneous thermal analysis

Simultaneous thermal analysis (STA) includes two typologies of tests executed at the same time: thermogravimetric analysis (TG) and differential scanning calorimetry (DSC). STA tests usually represent the preliminary step to obtain the kinetic properties through different methodologies: (i) analytical methods such as model fitting and model free [22]; (ii) inverse modelling, which combines pyrolysis models and numerical optimization methods [23, 24]. The calculation of kinetic properties being out of scope of this work, the data presented allow researchers to calculate them.

STA tests were carried out in NETZSCH STA 449 F3 Jupiter, and the samples were tested under different boundary conditions so as to analyse their effects over the samples, as it was analysed in [25]. To do so, the tests were executed using 2 values of initial mass (between 1 and 5 mg), 3 heating rates (5, 10 and 20 K $min^{-1}$) and 2 atmospheres (oxygen-content (20%) and non-oxygen-content). Every test was carried out at least two times to ensure the repeatability of the results. All tests were executed following the recommendations of the standards ISO 11358-1 [14] and ISO 11357–1 [15]. The crucibles employed were made of alumina ($Al_2O_3$ 99,7%) without lid, and the samples were chopped into small pieces. More details of these tests and samples are given in Table 1, in results section. Before running all tests, the STA apparatus was previously calibrated using reference material (gold) and following the procedure prescribed by the manufacturer.

## Laser flash analysis

The thermal decomposition process of any material under an external heat source is defined, among other properties, by its capacity to increase its inner temperature, i.e. the thermal inertia. Thermal inertia is a key factor that establishes how quickly increases the inner temperature of the material, and therefore, how long it takes for the decomposition process to begin. This factor is established by the following terms: density ($\rho$), thermal conductivity ($k$) and heat capacity ($C_p$). Thermal inertia ($I$) is calculated as Eq. 1 shows:

$$I = \sqrt{k \cdot C_p \cdot \rho} \tag{1}$$

Laser flash analysis (LFA) determines the diffusivity ($\propto$) of the material at selected temperature [26]. Thanks to the calculation of this parameter, and under certain conditions, heat capacity ($C_p$) can be also calculated [27]. The thermal conductivity ($k$) of the sample can estimated by the calculation of these two parameters. All three are related to the density ($\rho$) according to Eq. 2:

$$k = \propto \cdot \rho \cdot C_p \tag{2}$$

LFA tests were executed using NETZSCH LFA 447 NanoFlash. All circular samples were prepared according to [16], with a thickness of 2 mm and a diameter of 12.7 mm. The diffusivity was measured at 30, 80 and 130 °C. For every temperature, 10 laser pulses were triggered to ensure the repeatability of the results.

### Smoke density and toxicity

As far as visibility is concerned, the smoke density plays a major role since thick smoke causes low visibility situations and it could modify the egress of a building or mean of transport. A thick cloud of smoke can be generated in two unique ways: (i) the material burns massively; (ii) there is a large amount of smoke even though the amount of material burnt is small. While first point is assessed in cone calorimeter, the amount of smoke generated and its density are analysed through the smoke density test. The smoke density test provides the characteristic information about smoke production [28] using the variable $S_d$ (dimensionless). Two tests were executed according to ISO 5659-2 [17] using an external heat flux of 50 kW $m^{-2}$.

Not only does smoke density affect the egress, but also the toxicity of the fumes causes a large number of injuries and casualties [29, 30]. Therefore, smoke density test usually is carried out simultaneously with the toxicity test. The toxicity of fumes was measured using a Fourier transform infrared spectroscopy (FTIR) gas analyser by connecting the FTIR to the exhaust tube of the chamber where the smoke density tests were executed.

### Cone calorimetry

Cone calorimetry is the most relevant bench scale instrumentation in the field of fire testing. Cone calorimeter test evaluates the response of materials exposed to controlled levels of radiant heat flux, i.e. its easiness of ignition. Thanks to this test the following properties are measured: (i) ignition time; (ii) heat release rate (HRR); (iii) fire growth parameter (FIGRA); (iv) mass loss; (v) effective heat of combustion (EHC); (vi) total smoke produced (TSP); (vii) specific extinction area coefficient (SEA) and (viii) extinction coefficient or visible smoke (K). Although the heat flux can be

**Table 1** Features and results of STA tests and values from literature

| #Test/references | Features of the test | | | | | Results of the test | | | | | |
|---|---|---|---|---|---|---|---|---|---|---|---|
| | Initial mass/mg | HR/K $min^{-1}$ | Manufacturer/type | $O_2$ level/% | Gas flow/ mL $min^{-1}$ | Onset temp./°C | Mass loss/% 1st step | 2nd step | pMLR /% $°C^{-1}$ | Temp. pMLR /°C | Energy released/J $g^{-1}$ |
| #1 | 1.84 | 5 | P2MC | 20 | 60 | 385 | 81.95 | 13.92 | 0.40 | 403 | 2472 |
| #2 | 4.34 | 5 | P2MC | 20 | 60 | 384 | 85.90 | 11.87 | 0.47 | 414 | 2497 |
| #3 | 1.26 | 10 | P2MC | 20 | 60 | 394 | 85.80 | 9.52 | 0.69 | 422 | 2926 |
| #4 | 4.39 | 10 | P2MC | 20 | 60 | 401 | 88.55 | 9.04 | 0.40 | 394 | 2450 |
| #5 | 1.93 | 20 | P2MC | 20 | 60 | 411 | 90.58 | 6.73 | 0.14 | 419 | 2812 |
| #6 | 4.26 | 20 | P2MC | 20 | 60 | 413 | 90.75 | 7.03 | 0.23 | 394 | 2764 |
| #7 | 1.28 | 10 | P2MC | 0 | 60 | 408 | 95.84 | – | 0.62 | 437 | − 1157 |
| #8 | 1.23 | 10 | P2MC | 0 | 60 | 408 | 92.70 | – | 0.54 | 437 | − 1319 |
| [40] | 100% | 10 | 0215A | 20 | – | 390 | 85.51 | 4.72 | 2.30 | 410 | – |
| [41] | 5 | 10 | 0215A | 20 | 60 | 390 | 88.54 | 7.46 | 2.30 | 428 | – |
| [42] | 6–10 | 10 | D-120 | 20 | – | 395 | 88.98 | 10 | 2.65 | 435 | – |
| [43] | 2–10 | 20 | Cheil Industries | 20 | – | 351 | 81.86 | 9.95 | 2.48 | 430 | – |
| [33] | 20 | 10 | – | 0 | 40 | 385 | 96.84 | – | 1.90 | 425 | – |
| [46] | 100% | 10 | PA-757/Chimei | 20 | 60 | 355 | 87.50 | 10.56 | 1.94 | 523 | – |
| [40] | 100% | 10 | 0215A | 0 | – | 350 | 90.83 | – | 3.70 | 428 | – |
| [39] | < 10 | 10 | – | 0 | – | 377 | 99.50 | – | 0.30 | 432 | – |
| [44] | 100% | 10 | PA747 | 0 | – | 380 | 98.38 | – | 1.80 | 430 | – |
| [45] | 7 ± 0.1 | 10 | 0215A | 0 | – | 381 | 97.63 | – | 2.34 | 414 | – |
| [46] | 100% | 10 | PA-757/Chimei | 0 | 60 | 378 | 99.60 | – | 2.70 | 424 | – |
| [47] | < 10 | 10 | – | 0 | 50 | 385 | 98.67 | – | 0.32 | 432 | − 1460 |
| [48] | – | 10 | 727 Quimei | 0 | – | 393 | 96.2 | – | 1.92 | 432 | – |

selected up to 100 kW $m^{-2}$, heat fluxes are between 25 and 75 kW $m^{-2}$, being 50 kW $m^{-2}$ the most frequently one.

Following the procedure indicated in ISO 5660-1 [18], and using (FTT) Fire Testing Technology cone calorimeter, up to 4 tests were run with next features: (i) external heat flux of 50 kW $m^{-2}$; (ii) square samples with a dimensions of 100 × 100 × 2 mm; (iii) samples were wrapped with aluminium foil (except top face); and (iv) sample holder had a retainer frame for molten materials without grid. The initial mass was 21.8, 22.2, 22.5 and 22.3 g for Test #1 to #4, respectively. Due to the dimensions of the retainer frame, the total exposed area of the samples to the heat flux was 88.4 $mm^2$.

#### Propagation

Flame propagation can be defined as the affinity to spread of a flame away from the ignition source, and this determines substantially the fire hazard of a material. The FMVSS 302 (Federal Motor Vehicle Safety Standard) test [19] is employed for testing self-supporting flame and propagation flame of the polymers used in the interior of vehicles, as ABS does usually. Although this test should not be considered as a criterion for determining the fire risk of a material and obtaining a classification, is useful for analysing whether ABS meets minimum fire safety conditions or not.

FMVSS 302 is run by burning one edge of the sample and measuring the flame propagation speed and the total burnt length. The burn rate (*B*) is obtained measuring the time required to burn the distance from the edge up to the unburned zone. This test was run 3 times, as FMVSS 302 standard indicates, to confirm the repeatability of the results. The dimensions for all samples were 356 × 101.6 × 12.7 mm (length × width × thickness). Samples were tested in a tailor made apparatus following the standard [19] dimensions.

#### Flammability

Whether a material is involved or not in a fire depends on its capacity to ignite, i.e. its flammability. The flammability of a material is related directly with the ignition temperature [31], the less ignition temperature the more flammability. Flammability can be studied in two different ways: (i) observing the minimum temperature that triggers ignition ISO 871 [32] and (ii) analysing how the flame is extinguished once the external heat source disappears UL-94 [20]. UL-94 standard stablishes, as a preliminary classification, the easiness of polymers to burn. As FMVSS 302, UL-94 is helpful to classify the hazard of a material in a quick and easy way.

UL-94 test was repeated up to 4 times to assure the repeatability of the results. The dimensions of the samples were approximately 125 × 13 × 1.6 mm (length × width × thickness) and their initial mass was 2.818, 2.837, 2.790 and 2.778 g for Test #1–#4, respectively. These tests were run in a tailor made bench according to the standard [20] dimensions.

#### Limiting oxygen index

Limiting oxygen index (LOI) [21] test is another common method to evaluate the flammability of certain material. As UL-94, LOI test analyses the conditions to support a flaming combustion on a polymer after applying an external flame. During the test, the sample is placed inside a gas flow made of a mixture of oxygen and nitrogen with different concentration levels. LOI (in %) stands for the minimum oxygen concentration that would sustain a flaming combustion. Even though LOI tests were run in this work, LOI values are included from literature.

## Results

This section gathers the results from tests and literature organized in subsections with the same order as previous section.

#### Simultaneous thermal analysis

Figure 1a–d displays TG and DSC curves for all tests. Regardless the heating rate and atmosphere, the range of onset temperatures, i.e. when the thermal decomposition process is triggered, has values between 384 and 413 °C. On the one hand, in oxygen-content atmosphere (Fig. 1a), the decomposition process had two steps: first one up to 490 °C, and second one from 490 to 590 °C approximately. On the other hand, in non-oxygen-content atmosphere (Fig. 1b) only one step was observed between 370 and 500 °C.

As far as energy released is concerned, when the thermal decomposition process took place in oxygen-content atmosphere (Fig. 1c), there were two exothermic peaks caused by two mass-loss steps. In every heating rate, second peak had higher values than first one, i.e. more energy was released during the second decomposition step. A relationship between heating rate and energy produced was observed, i.e. the highest heating rates, the highest peaks of energy produced. Nevertheless, the total amount of energy released remained within the range between 2450 and 2926 J $g^{-1}$. When the decomposition processes occurred in non-oxygen-content (Fig. 1d), there were two endothermic peaks (at 430 °C and 680 °C approximately), with the first peak being greater than the second one. It can be appreciated that the second peak was not linked to a mass-loss process as in oxygen-content atmosphere does. Without oxygen, the energy absorbed had values between − 1319 and − 1157 J $g^{-1}$.

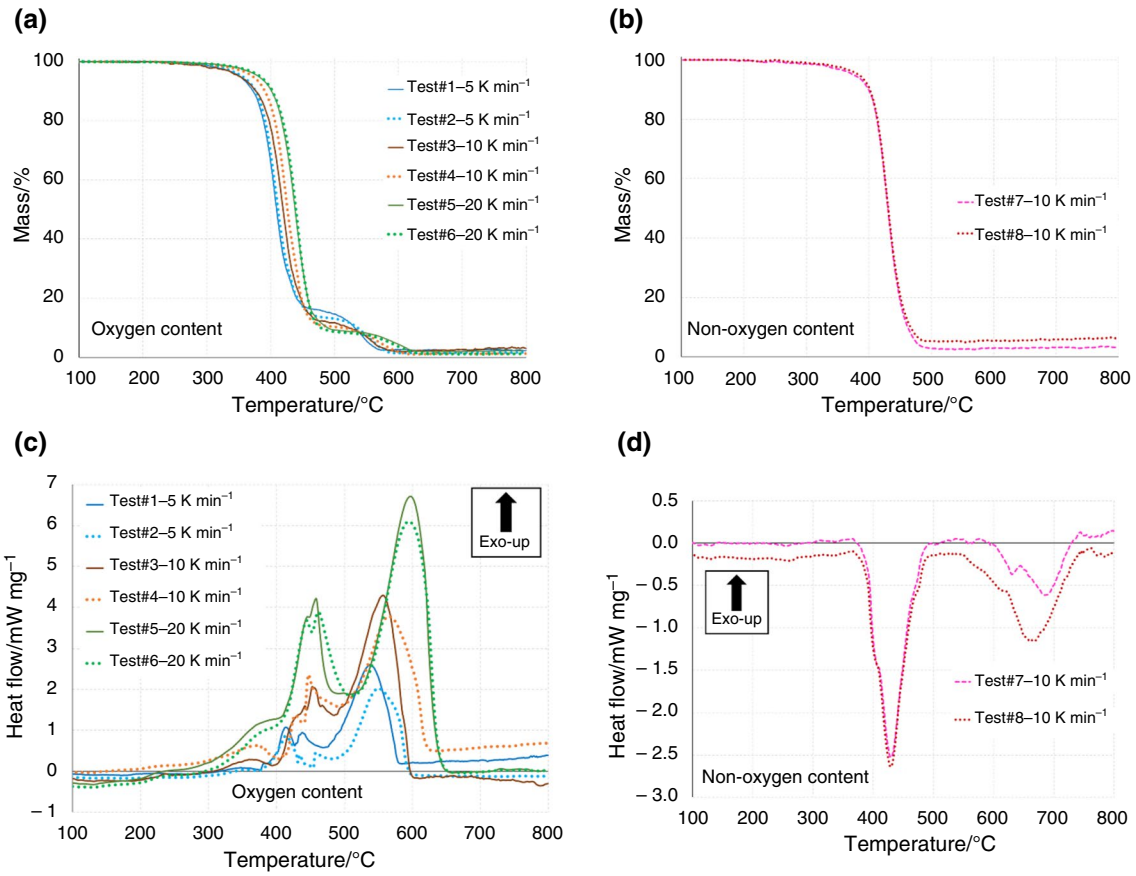


**Fig. 1** Results of STA tests: **a** mass curves (TG) in oxygen-content atmosphere; **b** mass curves (TG) in non-oxygen-content atmosphere; **c** heat flow curves (DSC) in oxygen-content atmosphere; **d** heat flow curves (DSC) in non-oxygen-content atmosphere

Numerous studies can be found in the literature concerning the thermal analysis of neat ABS and ABS blends. Among others, we can highlight [33–48] and their results will be analysed and compared with the results from the experimental campaign developed in this work below.

Figure 2 shows the comparison between experimental results from tests and literature. To stablish a suitable comparison, we selected from literature those works testing neat ABS with same boundary conditions, i.e. same heating rate and same atmosphere (10 K $min^{-1}$ in both atmospheres and

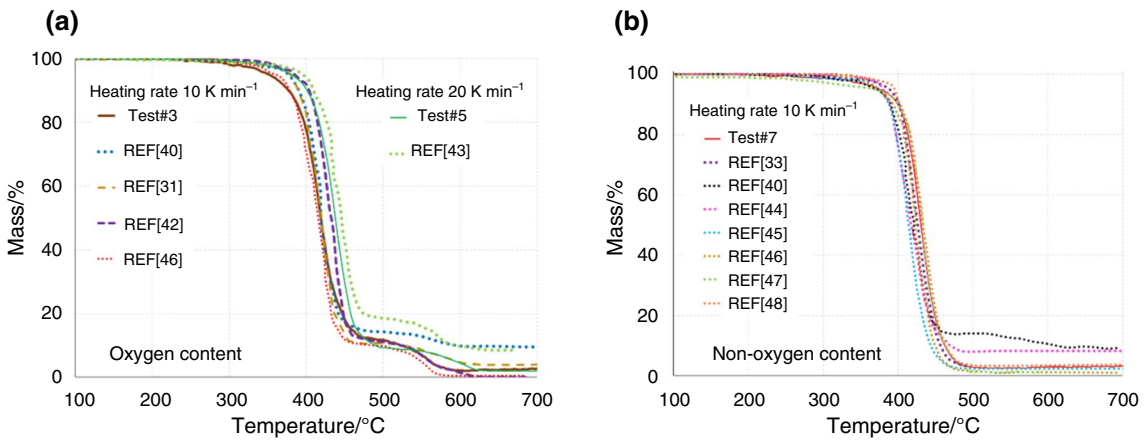


**Fig. 2** Mass curves (TG) comparison, experimental (solid lines) vs. literature: **a** oxygen-content atmosphere; **b** non-oxygen-content atmosphere

20 K $min^{-1}$ for oxygen contain atmosphere only). Table 1 compares the tests and literature including next features: (i) the initial mass; (ii) heating rate (HR); (iii) reference or manufacturer; (iv) onset temperature; (v) mass loss; (vi) mass-loss rate (MLR), its main peak (pMLR) and the temperature when is produced; (vii) energy released (area between DSC curve and X-axis). Unfortunately, not all parameters from the literature could be included because they were not mentioned in the original paper, thus missing values are marked with "–".

For all experimental tests, the onset temperatures were within a range between 350 and 413 °C. From 400 up to 450 °C approximately, slight differences were observed, and could be caused mainly by the heating rate and the initial amount of mass. Finally, from 450 °C up to 700 °C, the atmosphere produced the most remarkable difference. Whereas in oxygen-content atmosphere the mass continued to decrease but at different rate, in non-oxygen-content atmosphere the mass-loss process was about finished. In sum, within oxygen-content atmosphere, the thermal degradation was produced in two steps, while in non-oxygen-content atmosphere; it took place in one step only. Even though same material and heating rates were compared, Fig. 2 shows slight differences between results. We discuss the origin of these differences in conclusion section.

## Laser flash analysis

Table 2 displays the results obtained for the diffusivity. These values represent the average value of 10 pulses for each temperature. Furthermore, Table 2 includes the calculated values for heat capacity, thermal conductivity and thermal inertia [calculated using Eq. (1)]. All parameters are compared with those from literature.

On the one hand, values of the diffusivity decreased with the increasing of the temperature. On the other hand, heat capacity and thermal diffusivity increased when the temperature does. There are no many works concerning LFA tests of neat ABS in literature. Nevertheless, the values of heat capacity and thermal conductivity obtained from tests were similar to those available in literature. Diffusivity experimental values were similar to those achieved in [49–51]. Regarding the heat capacity and the thermal conductivity, the experimental values were similar to those found in [51–54].

## Smoke density and toxicity

Next Fig. 3 and Table 3 show the results of smoke density and toxicity from the two tests carried out. Both samples generated the same amount of smoke density ($S_d$) and they had similar behaviour since the mass loss, ignition and

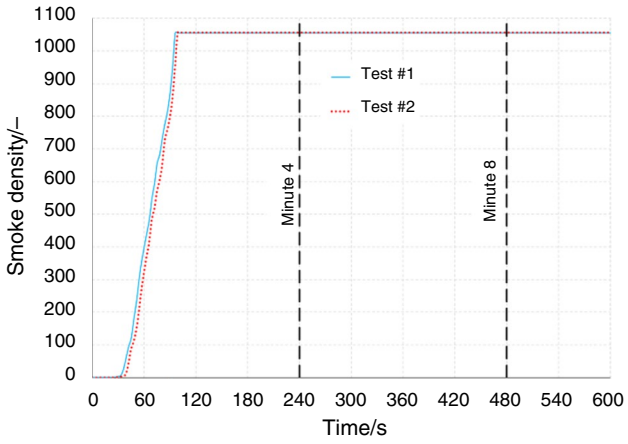


**Fig. 3** Results of smoke density ($S_d$) tests

**Table 2** Average values of measured and calculated properties in LFA tests and values from literature

| #Test/references | Sample shape (round square) | Manufacturer/type | Temp./°C | Diffusivity/ $mm^2\ s^{-1}$ | Heat capacity/J/ $g^{-1}\ K^{-1}$ | Thermal conductivity/W/ $m^{-1}\ K^{-1}$ | Thermal inertia/ kJ $m^{-2}\ K^{-1}\ s^{-1/2}$ |
|---|---|---|---|---|---|---|---|
| #1 | *R* | P2MC | 30 | 0.114 | 1.235 | 0.149 | 1131.901 |
| #2 | *R* | P2MC | 80 | 0.106 | 1.443 | 0.161 | 1658.933 |
| #3 | *R* | P2MC | 130 | 0.083 | 2.039 | 0.174 | 3475.806 |
| [49] | – | Borg-Warner Chemicals Inc | – | 0.078 | – | 0.166 | – |
| [50] | *R* (10×10×4 mm) | – | – | 0.140 | – | – | – |
| [51] | – | – | – | 0.112 | 1.450 | 0.193 | – |
| [52] | – | – | – | – | 1.484–1.938 | – | – |
| [53] | – | ABS melt flow index 20 | – | – | 0.628–1.758 | – | – |
| [54] | S (Ø10 mm) (2 mm thickness) | MG94 | – | – | 1.381 | 0.173 | – |

**Table 3** Results of smoke density ($S_d$) tests

| Test | Thickness/mm | Initial mass/g | Final mass/g | Ignition time/s | Extinction time/s | $S_d$ at minute 4/- | $S_d$ at min 8 | $S_d$ max |
|---|---|---|---|---|---|---|---|---|
| #1 | 11.7 | 11.7 | 0.2 | 30 | 579 | 1056 | 1056 | 1056 |
| #2 | 2.1 | 12.0 | 0.3 | 33 | 600 | 1056 | 1056 | 1056 |

extinction time were almost identical. Unfortunately, no reference of smoke density test concerning neat ABS was found in literature so as to compare the results.

Table 4 summarizes the concentration of the species and the range of the temperatures they reached. The measurements were acquired punctually at 4 and 8 min. After testing the samples 2 times, we found similar values of gases concentration after 4 and 8 min. The smoke of the first test was warmer than in second test.

### Cone calorimetry

Figure 4 shows the curves obtained in experimental the tests and their averages curves: (a) HRR; (b) mass (normalized); (c) effective heat of combustion (EHC); (d) extinction coefficient (K); (e) total smoke production (TSP) and (f) specific smoke extinction area (SEA). Table 5 summarizes the relevant values of the results.

All samples loss their mass completely. As average value, ABS ignites at 28 s and the flameout was produced after 115 s. As ISO 13943 indicates [31], the ignition time should be taken into account only as reference since this value is influenced by test conditions. The average value of heat release peak was about 1081.4 kW $m^{-2}$ and took place 78 s (as average) after beginning of the test.

In literature, we can find several works testing neat ABS under a same external flux (50 kW $m^{-2}$) [37, 48, 55–63]. We would like to highlight the works of [47] and [61] since these works tested ABS with different oxygen concentration level. These works employed a modification cone known as controlled atmosphere cone calorimeter (CACC) or controlled atmosphere pyrolysis apparatus (CAPA). CACC or CAPA is a cone calorimeter modified that allows testing in different oxygen concentrations. These tests are not common for cone calorimeter tests, and they intend to clarify the determination of combustion regimes basis on the oxygen concentration. Furthermore, thanks to these tests, during the process of modelling process, it is expected to minimize errors and extend the scope of the model's validity [64]. Therefore, the data obtained in different oxygen concentration are useful to make a comparison between oxygen-content and non-oxygen-content atmosphere and to observe the effects of the lack of oxygen. In [65], authors have also studied the effect of the flame during combustion in cone calorimeter modifying the sample holder and analysing how the heat flux affect the ABS as a function of the decomposition and the combustion processes.

Not only can a heat flux of 50 kW $m^{-2}$ be used for cone calorimeter test, but also there are other works using different levels. For instance, in [6, 38, 40, 66–69] a value of 35 kW $m^{-2}$ was used; in [70] the authors employed 20, 40 and 70 kW $m^{-2}$, and in [58] 50 and 75 kW $m^{-2}$ were used.

HRR curve provides an overall information about the fire behaviour of the sample; therefore, most papers include it. Figure 5 compares HRR curves from tests (average value) and from quoted literature. HRR curves from literature were

**Table 4** Species measured by FTIR gas analyser from smoke density and toxicity tests

| Gas | Test #1 | | Test #2 | |
|---|---|---|---|---|
| | 4 min | 8 min | 4 min | 8 min |
| Carbon dioxide ($CO_2$)/ppm | 20,918.2 | 23,194.1 | 21,858.13 | 23,126.73 |
| Carbon monoxide (CO)/ppm | 1141.2 | 1237.6 | 1217.84 | 1304.14 |
| Nitrogen monoxide (NO)/ppm | 167.6 | 166.41 | 182.2 | 196.98 |
| Nitrogen dioxide ($NO_2$)/ppm | 0.65 | 2.08 | 0.13 | 1.09 |
| Sulphur dioxide ($SO_2$)/ppm | 9.35 | 5.74 | 10.17 | 10.63 |
| Hydrogen chloride (HCl)/ppm | 0.4 | 0 | 0 | 0 |
| Hydrogen fluoride (HF)/ppm | 0 | 0 | 0 | 0 |
| Hydrogen cyanide (HCN)/ppm | 69.15 | 72.65 | 80.36 | 82.18 |
| Hydrogen bromide (HBr)/ppm | 7.93 | 15.34 | 6.1 | 8.91 |
| $NO_x$/ppm | 168.25 | 168.49 | 182.33 | 198.07 |
| Range of temperatures of the smoke produced/°C | 103.7 ÷ 105.9 | | 100.8 ÷ 100.9 | |

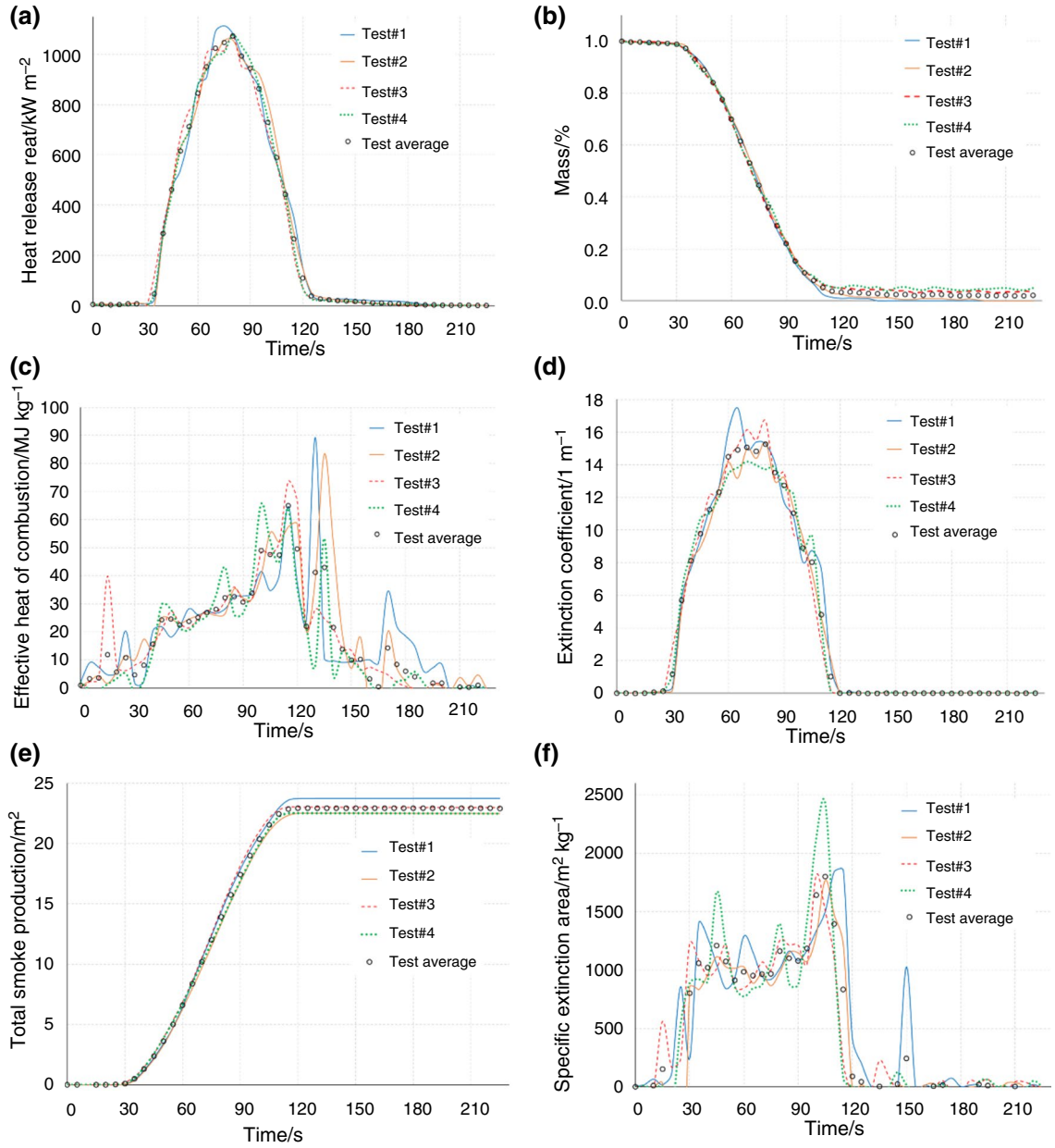


**Fig. 4** Results of cone calorimeter tests: **a** heat release rate; **b** mass loss (normalized); **c** effective heat of combustion; **d** extinction coefficient; **e** total smoke produced; **f** specific extinction area coefficient

obtained with same boundary conditions and material, i.e. an external flux of 50 kW $m^{-2}$ and neat ABS. Furthermore, it is also included the results from [61] with an oxygen level of 12.5% $O_2$ plotted in blue dotted line.

Although all samples were made of neat ABS, there was a certain degree of divergence in the results. The average experimental curve matched with most of the curves from literature up to approximately 50 s. After this moment, the experimental average curve was similar to [63] curve only, up to HRR peak was reached. Among the curves form literature, there were similarities between most of them, with some exceptions such as [58, 60, 63]. While time to ignition was similar, around 30 s, HRR peaks and time when they took place were different. Nevertheless, most of tests produced a peak HRR of about 1000 kW $m^{-2}$ and took place between 78 and 150 s. As for the duration of the tests, there were differences due to different initial amount of mass and thickness of the samples. These two properties could modify

**Table 5** Cone calorimeter results

| Measurement | Test #1 | Test #2 | Test #3 | Test #4 | Average |
|---|---|---|---|---|---|
| Initial mass/g | 21.80 | 22.20 | 22.50 | 22.30 | 20.20 |
| Total mass loss/g | 21.68 | 21.97 | 21.61 | 21.11 | 21.59 |
| Ignition time/s | 29 | 29 | 26 | 28 | 28 |
| Flameout time/s | 117 | 117 | 114 | 115 | 116 |
| HRR peak/kW $m^{-2}$—(time peak/s) | 1114.3 (75) | 1057.4 (80) | 1076.4 (80) | 1077.3 (80) | 1081.4 (79) |
| FIGRA/kW $m^{-2}$ $s^{-1}$ | 14.8 | 13.2 | 13.4 | 13.4 | 13.7 |
| MLR peak/g $s^{1}$—(time peak/s) | 0.42 (70) | 0.40 (75) | 0.40 (75) | 0.45 (60) | 0.42 (70) |
| EHC peak/MJ kg—(time peak/s) | 89.2 (130) | 83.4 (135) | 73.7 (115) | 65.5 (100) | 77.9 (120) |
| K peak/1 $m^{-1}$—(time peak/s) | 17.4 (65) | 16.8 (80) | 16.6 (80) | 14.1 (70) | 16.3 (73) |
| SEA peak/$m^2$ $kg^{-1}$—(time peak/s) | 1852.3 (115) | 1769.5 (105) | 1811.7 (100) | 2427.0 (105) | 1965.1 (106) |

the shape of the HRR curve, changing the value of peak and the peak width.

Table 6 includes the results from experimental tests (average values) and from quoted works that employ same heating rate. As some original works did not include the request value, some fields of this table are marked as "–". Besides, Table 6 includes other characteristics that helps to define the samples employed such as shape, pigmentation, grid and denomination of the polymer.

### Propagation

Table 7 shows the results from propagation tests according to FMVSS 302 standard. The control points, established by this standard, represent the distances between them and the edge where the fire starts. The gaps between the edge and control points were 38, 165 and 292 mm for 1st, 2nd and 3rd point, respectively. The times displayed in the table indicates the moment when the flame front reached each control point, whereas the burn rate indicates the front-flame propagation velocity.

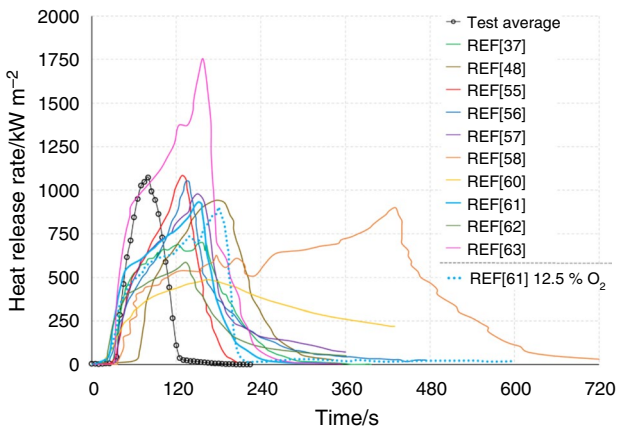


**Fig. 5** Comparison of HRR experimental average curves achieved from tests and from literature

Even though for the 1st control point of Test #2 there was an noticeable difference, similar times between tests were obtained. As average, a burn rate of 36 mm/min was observed. Regarding propagation test, in [71] authors analysed up to 48 materials from parts used inside and outside the passenger car, among them the neat ABS. It was found a value of 33.02 mm $min^{-1}$ for the burn rate, which was similar to the value of Test #3 and diverged up to 5 mm $min^{-1}$ from Test #1.

### Flammability

All tests carried out produced flaming drops, hence, according to [20], when the specimen drips flaming particles the material obtains "No Rated-NR" class, i.e. the material does not achieve the minimum requirements to obtain even the lowest category. The neat ABS is an easily flammable polymer, as it was expected. The results from literature classified the neat ABS as "NR"; however, in [62] the ABS measured by the authors burnt completely and obtained the "HB" class, which implies "Slow burning".

Table 8 summarizes the classification obtained, the event that produces that classification and the instant when it takes place.

### Limiting oxygen index

Table 9 gathers the LOI limits measured from literature. Having obtained an average value of 18.3% of oxygen concentration to support a flame during its combustion, ABS can easily maintain a flame under normal atmospheric conditions.

**Table 6** Cone calorimeter results under heat flux of 50 kW $m^{-2}$: experimental tests (average) and literature

| Measurement | Test average | [37] | [48] | [55] | [56] | [57] |
|---|---|---|---|---|---|---|
| Initial mass/g | 20.20 | 35.00 ± 3 | – | – | – | – |
| Thickness/mm | 2.0 | 3.3 | – | – | 3.2 | – |
| Shape (square/round) | S | S | S | – | S | – |
| Side—diameter/mm | 100 | 100 | 100 | – | 100 | – |
| Pigmentation | No | – | – | – | – | – |
| Denomination | P2MC | 0215 A | 727 Qimei | PA-757 | GP22, BASF | – |
| Sample set-up/underneath sample insulation | Wrapped with aluminium foil/ceramic fibre | – | – | – | Wrapped with aluminium | – |
| Top grid | No | No | – | – | – | – |
| Total mass loss/g | 21.59 | 76% | – | – | – | – |
| Ignition time/s | 28.0 | 21.0 | 65.0 | 27.0 | 24.0 | 32.0 |
| Flameout time/s | 115 | – | 343 | – | – | – |
| HRR peak/kW $m^{-2}$—(time peak/s) | 1081–78 | 698–162 | 951–178 | 1078–128 | 1016–137 | 980–150 |
| FIGRA/kW $m^{-2}$ $s^{-1}$ | 13.70 | 4.90 | 5.34 | 8.40 | 6.50 | 9.20 |
| MLR peak/g $s^{-1}$—(time peak/s) | 0.42–70 | – | 0.096 | – | – | – |
| EHC peak/MJ $kg^{-1}$—(time peak/s) | 77.90–120 | 73.7/– | – | – | – | – |
| K peak/1 $m^{-1}$—(time peak/s) | 16.20–72 | – | – | – | – | – |
| SEA peak/$m^2$ $kg^{-1}$—(time peak/s) | 1965–106 | – | – | – | – | – |
| Measurement | [58] | [59] | [60] | [61] | [62] | [63] |
| Initial mass/g | 10.65 | 33.00 ± 0 | 39.39 | 32.09 ± 0.15 | – | – |
| Thickness/mm | 10.0 | 3.3 | 4.0 | 3.0 ± 0.03 | 4.0 | 5.0 |
| Shape (square/round) | S | S | S | S | S | S |
| Side—diameter/mm | 100 | 100 | 100 | 100 | 100 | 100 |
| Pigmentation | – | – | – | White | – | – |
| Denomination | $C_8H_8$-$C_4H_6$-$C_3H_3N$ | Terluran GP-35 INEOS Styrolution | Recycled ABS | POLYPENCO 42,400,104/3 MM | Çrocadur RABS 52 | ELIX 128 IG |
| Sample set-up/underneath sample insulation | Wrapped with aluminium foil/ceramic fibre | – | – | Aluminium foil/silica wool | Aluminium foil/– | – |
| Top grid | – | No | – | No | – | – |
| Total mass loss/g | – | – | 38.75 | –- | 99.26% | 99.48 |
| Ignition time/s | 49.0 | 32.0 ± 2 | 15.0 | 20.7 ± 1.5 | 24.0 | 32.0 |
| Flameout time/s | – | – | 430 | 330 | 361 | |
| HRR peak/kW $m^{-2}$—(time peak/s) | 970/430 | 1509 ± 13/–- | 486/165 | 993/152 | 486.05/152 | 1760/156 |
| FIGRA/kW $m^{-2}$ $s^{-1}$ | 2.80 | – | – | – | 3.45 | – |
| MLR peak/g $s^{-1}$—(time peak/s) | 0.31–431 | – | 0.2–165 | 0.77–139 | – | – |
| EHC peak/MJ $kg^{-1}$—(time peak/s) | – | – | 14.85- - | – | – | – |
| K peak/1 $m^{-1}$—(time peak/s) | – | – | – | – | – | – |
| SEA peak/$m^2$ $kg^{-1}$—(time peak/s) | – | – | – | – | – | – |

**Table 7** Results of the propagation tests

| Measurement | Test #1 | Test #2 | Test #3 | Average | [71] |
|---|---|---|---|---|---|
| 1st control point—time to reach/s | 99 | 51 | 92 | 81 | – |
| 2nd control point—time to reach/s | 293 | 273 | 314 | 293 | – |
| 3rd control point—time to reach/s | 499 | 482 | 543 | 508 | – |
| Burn rate ($B$)/mm $min^{-1}$ | 38.00 | 35.00 | 34.00 | 36.00 | 33.02 |

**Table 8** Results of the UL-94 flammability tests

| Test/references | Manufacturer | Event | Time (s) | Classification |
|---|---|---|---|---|
| #1 | P2MC | Sample falls and burns the cotton | 36 | NR |
| #2 | P2MC | Sample falls and burns the cotton | 29 | NR |
| #3 | P2MC | First drop falls and burns the cotton | 16 | NR |
| #4 | P2MC | First drop falls and burns the cotton | 27 | NR |
| [4] | Cheil industries | – | – | NR |
| [35] | Terluran GP-22, BASF | – | – | NR |
| [37] | 0215 A | – | – | NR |
| [38] | 0215 A | – | – | NR |
| [46] | PA-757 Chimei | – | – | NR |
| [48] | 727 Qimei | Dripping | – | NR |
| [55] | PA-757 | – | – | NR |
| [56] | GP22, BASF | – | – | NR |
| [62] | Rocadur RABS 52 | Burning drops | – | HB |
| [63] | ELIX 128IG | Flammable drips | – | NR |
| [68] | PA-757 K | – | – | NR |
| [72] | ELIX 128IG | – | – | NR |
| [73] | – | – | – | NR |
| [74] | PA-747, Qimei Industry Stock Limited Company | – | – | NR |
| [75] | Cheil industries | – | – | NR |

**Table 9** Results of LOI tests from literature

| References | Manufacturer | LOI / vol% |
|---|---|---|
| [4] | Cheil industries | 18.3 |
| [35] | Terluran GP-22, BASF | 19.0 |
| [37] | 0215 A | 18.0 |
| [38] | 0215 A | 18.4 |
| [46] | PA-757 Chimei | 18.5 |
| [48] | 727 Qimei | 18.0 |
| [55] | PA-757 | 18.7 |
| [56] | GP22, BASF | 19.0 |
| [62] | Rocadur RABS 52 | 18.5 |
| [68] | PA-757 K | 18.2 |
| [76] | – | 17.8 |
| [70] | Cycolac CTB ABS terpolymer (Borg-Warner) | 17.6 |
| [72] | ELIX 128IG | 18.0 |
| [75] | Cheil industries | 18.4 |
| [77] | Cheil industries (18 mass% butadiene, 35.9 mass% acrylonitrile) | 18.5 |
| [78] | – | 18.3 |

## Conclusions and discussions

This work shows the results of different types of laboratory tests carried out on neat ABS and compare them with results from other relevant works from literature. Through these two approaches, this paper aims to present a comprehensive characterization of neat ABS fire behaviour: (i) providing a comprehensive baseline for the comparison between neat and blended ABS; (ii) enhancing similarities and differences in results due to experimental set-up. Despite testing the same material using similar boundary conditions, some differences have been found.

Regarding STA tests, as a function of atmosphere and the heating rate, TG and DSC different curves were obtained, as it has already observed in [25, 42]. Nonetheless, despite using same atmosphere and heating rate, some differences arose between curves. For instance, in Fig. 2a at 10 K $min^{-1}$, there were discrepancies in onset temperature and final amount of residue. While in Test #3 and Test #4 the onset temperature were 394 and 401 °C, respectively, in literature the values found were 385 °C in [33], 390 °C in [40, 41] and 395 °C in [42]. Regarding the residue, Test #3 and #4 left 4.68% and 2.41%, respectively, and among the quoted references were found values of 9.77, 4.00 and 1.02% for [40–42], respectively. These differences could be originated due to the origin of the material because they come from different manufactures and the different initial amount of its components. The thermal degradation of the ABS is accepted to be the sum of several overlapped processes that produce one single-step reaction [79], alike end-chain and random-chain scissions. The small differences found are directly related to the initial butadiene content. While the degradation of the butadiene started about 340 °C and the styrene at 350 °C, the acrylonitrile began at 400 °C [80]. Nonetheless, under

non-oxygen-content atmosphere, the mass-loss process happened in one step, between 350 °C and 500 °C. In this range of temperatures, the pyrolysis of the main chain was produced [80]. Other factors such as gas flow are unknown as well, except for [33, 41, 46, 47], and they may have influence on the results. In [25], the effects of boundary conditions in STA tests were analysed concluding that boundary conditions such as initial mass, gas flow, etc. have influence in TG and DSC curves. Therefore, it seems to be important define the boundary conditions of STA and provide them in publications so as to have a complete information about the test set-up.

As far as LFA tests are concerned, the results from tests and from literature show slight differences. As the diffusivity ($\propto$), heat capacity ($C_p$) and thermal conductivity ($k$) are dependent on the temperature, the differences could be explained due to test temperatures. There are few works in literature for neat ABS and those available do not specify the temperature at which the test was run. This lack of information about boundary conditions could mislead the readers; therefore, to improve the quality of the data, it is recommended to provide a full description of the test, e.g. temperatures where the tests are carried out, sample dimensions and manufacturer.

As for cone calorimeter tests, as sample sizes increase, the discrepancies between results became even more significant. Although test results in this work achieved a good degree of repeatability, when they were compared under similar circumstances with the literature ones, there were some differences. Whereas time to ignition and HRR peaks had a certain degree of coincidence (except [58, 60, 62, 63]), FIGRA, time to HRR peak, and duration of tests had a wide range of values. These differences could stem from point similar to those identified in STA tests. For instance, the thickness of the sample, its shape (square or round), the configuration of the unexposed face of the sample (insulation or not) and the fact of manufacturers produce the ABS adding components in different concentrations [79]. The effect of the sample thickness has already analysed in [81] (chapter 26) for the polymethyl methacrylate (PMMA) and found to be a significant feature of sample behaviour. All in all, these aspects may modify the total amount of heat flux received and reflected by the sample, therefore, how this heat flux behaves within the sample as [82] describes. In addition, as the samples analysed in this type of test are larger, the differences between works from references are more significant than in STA and LFA tests. Despite this circumstance, not all works report all information, which would be useful to explain the differences. Table 6 shows how the samples compared have different thickness, shape and sample insulation; therefore, the results are affected.

The results concerning propagation revealed no significant differences between essays and literature.

The flammability was studied using two types of tests: UL-94 and LOI. While UL-94 provides quality results, LOI gives quantity results. For this reason, the results of UL-94 tests and literature had similar outcome, i.e. “No-Rated”. It means that neat ABS is highly flammable, as a result, this polymer usually blended with flame retardants. On the other hand, although the dimensions of the sample and the test procedure [21] does not allow many differences, LOI tests obtained different values. The minimum oxygen index values were between 17.6 and 19.0%. These differences could stem from the origin of the ABS, i.e. the chemical composition of the ABS.

On the whole, the differences highlighted in this paper support the idea that providing full details about sample and test set-up, as far as possible, would make the comparison between works more suitable. It would also mean less divergence in results due to more similar materials and test characteristics are compared. These features are useful for researchers to know how experiments are conducted and whether they agree with the boundary conditions the researchers are looking for.

Thanks to the data and properties listed in results section, this work stands for a useful baseline for any future alteration of neat ABS, representing an starting point to make a comparison between neat one and mixed ones.

**Acknowledgements** This work has been previously presented in 1st Central and Eastern European Conference on Physical Chemistry & Materials Science (CEEC-PCMS1). The authors would like to thank the organisation for their collaboration. Authors would like to thank to FLASH Project funded by FEDER/Ministerio de Ciencia, Innovación y Universidades—Agencia Estatal de Investigación/Proyecto RTC-2017-6414-5.

**Funding** Open Access funding provided thanks to the CRUE-CSIC agreement with Springer Nature.



## References

1. Geyer R, Jambeck JR, Law KL. Production, use, and fate of all plastics ever made. Production, use, and fate of all plastics ever made. Sci Adv. 2017;7:e1700782. https://doi.org/10.1126/sciadv.1700782.

2. Acrylonitrile Butadiene Styrene (ABS) Market share, size & trend analysis report. Source: application and segment forecasts to 2024. 2018. https://www.grandviewresearch.com/industry-analysis/acrylonitrile-butadiene-styrene-market. Accessed 30 Sep 2022
3. Ramirez NV, Sanchez-Soto M. Effects of poss nanoparticles on ABS-g-Ma thermo oxidation resistance. Polym Compos. 2012;33(10):1707–18. https://doi.org/10.1002/pc.22304.
4. Hoang D, Kim W, An H, Kim J. Flame retardancies of novel organo-phosphorus flame retardants based on DOPO derivatives when applied to ABS. Macromol Res. 2015;23(5):442–8. https://doi.org/10.1007/s13233-015-3058-5.
5. Shoulberg RH. The thermal diffusivity of polymer melts. J Appl Polym Sci. 1963;7(5):1597–611. https://doi.org/10.1002/app.1963.070070503.
6. Zhong H, Wei P, Jiang P, Wang G. Thermal degradation behaviors and flame retardancy of PC/ABS with novel silicon-containing flame retardant. Fire Mater. 2007;31(6):411–23. https://doi.org/10.1002/fam.953.
7. Morgan AB, Bundy M. Cone calorimeter analysis of UL-94 V-rated plastics. Fire Mate. 2007;31(4):257–83. https://doi.org/10.1002/fam.937.
8. Leventon I, Batiot B, Bruns M, Hostikka S, Nakamura Y, Reszka P, Rogaume T, Stoliarov S. The MaCFP condensed phase working group: a structured, global effort towards pyrolysis model development. In: Symposium on obtaining data for fire growth models. Atlanta: ASTM Selected Technical Papers (STP); 2021.
9. Alonso A, Lázaro D, Lázaro M, Alvear D. Self-heating evaluation on thermal analysis of polymethyl methacrylate (PMMA) and linear low-density polyethylene (LLDPE). J Therm Anal Calorim. 2022. https://doi.org/10.1007/s10973-022-11364-x.
10. Martinka J, Rantuch P, Sulová J, Martinka F. Assessing the fire risk of electrical cables using a cone calorimeter. J Therm Anal Calorim. 2019;135(6):3069–83. https://doi.org/10.1007/s10973-018-7556-5.
11. Elix ABS P2MC Data Sheet. https://www.elix-polymers.com/. Accessed 30 Sep 2022.
12. Tewarson A. Flammability parameters of materials: ignition, combustion, and fire propagation. J Fire Sci. 1994;12(4):329–56. https://doi.org/10.1177/073490419401200.
13. Ozawa T. Thermal analysis—review and prospect. Thermochim Acta. 2000;355(1–2):35–42. https://doi.org/10.1016/s0040-6031(00)00435-4.
14. ISO 11358-1:2022. Plastics—thermogravimetry (TG) of polymers—part 1: general principles. 2022. https://www.iso.org/standard/79999.html. Accessed 30 Sep 2022.
15. ISO 11357-1:2016. Plastics—differential scanning calorimetry (DSC)—part 1: general principles. 2016. https://www.iso.org/standard/70024.html. Accessed 30 Sep 2022.
16. ASTM E1461-13. Standard test method for thermal diffusivity by the flash method. West Conshohocken: ASTM International; 2022. https://doi.org/10.1520/E1461-13R22
17. ISO 5659-2:2017. Plastics—smoke generation—part 2: determination of optical density by a single-chamber test. 2017. https://www.iso.org/standard/65243.html. Accessed 30 Sep 2022.
18. ISO 5660-1:2015. Reaction-to-fire tests—heat release, smoke production and mass loss rate—part 1: heat release rate (cone calorimeter method) and smoke production rate (dynamic measurement). 2015. https://www.iso.org/standard/57957.html. Accessed 30 Sep 2022.
19. Flammability of Interior Materials. Federal motor vehicle safety standard no. 302 (FMVSS 302). U.S. Department of transportation. National Highway Traffic Safety Administration-NHTSA; 1991. https://www.govinfo.gov/app/details/CFR-2011-title49-vol6/CFR-2011-title49-vol6-sec571-302 Accessed 30 Sep 2022.
20. UL-94. Standard for tests for flammability of plastic materials for parts in devices and appliances. Underwriters Laboratories Inc; 2013. https://standardscatalog.ul.com/ProductDetail.aspx?productId=UL94. Accessed 30 Sep 2022.
21. ASTM D2863-19. Standard test method for measuring the minimum oxygen concentration to support candle-like combustion of plastics (oxygen index). West Conshohocken: ASTM International; 2019. https://doi.org/10.1520/D2863-19.
22. Lázaro D, Alonso A, Lázaro M, Alvear D. A simple direct method to obtain kinetic parameters for polymer thermal decomposition. Appl Sci. 2021;11(23):11300. https://doi.org/10.3390/app112311300.
23. Ira J, Hasalová L, Šálek V, Jahoda M, Vystrčil V. Thermal analysis and cone calorimeter study of engineered wood with an emphasis on fire modelling. Fire Technol. 2019;56(3):1099–132. https://doi.org/10.1007/s10694-019-00922-9.
24. Alonso A, Lázaro M, Lázaro P, Lázaro D, Alvear D. LLDPE kinetic properties estimation combining thermogravimetry and differential scanning calorimetry as optimization targets. J Therm Anal Calorim. 2019;138(4):2703–13. https://doi.org/10.1007/s10973-019-08199-4.
25. Lázaro D, Lázaro M, Alonso A, Lázaro P, Alvear D. Influence of the STA boundary conditions on thermal decomposition of thermoplastic polymers. J Therm Anal Calorim. 2019;138(4):2457–68. https://doi.org/10.1007/s10973-019-08787-4.
26. Parker WJ, Jenkins RJ, Butler CP, Abbott GL. Flash method of determining thermal diffusivity, heat capacity, and thermal conductivity. J Appl Phys. 1961;32(9):1679–84. https://doi.org/10.1063/1.1728417.
27. Marinelli G, Martina F, Lewtas H, Hancock D, Mehraban S, Lavery N, Ganguly S, Williams S. Microstructure and thermal properties of unalloyed tungsten deposited by Wire + Arc Additive Manufacture. J Nucl Mater. 2019;2019(522):45–53. https://doi.org/10.1016/j.jnucmat.2019.04.049.
28. Chen X, Jiang Y, Jiao C. Smoke suppression properties of ferrite yellow on flame retardant thermoplastic polyurethane based on ammonium polyphosphate. J Hazard Mater. 2014;266:114–21. https://doi.org/10.1016/j.jhazmat.2013.12.025.
29. Fahy RF, Molis JL. Firefighter fatalities in the United States 2018. NFPA—National Fire Protection Association; 2019. https://www.nfpa.org/-/media/Files/News-and-Research/Fire-statistics-and-reports/Emergency-responders/2019FFF.ashx. Accessed 30 Sep 2022.
30. Stec AA. Fire toxicity—The elephant in the room? Fire Saf J. 2017;91:79–90. https://doi.org/10.1016/j.firesaf.2017.05.003.
31. ISO 13943:2017. Fire safety—vocabulary. 2017 https://www.iso.org/standard/63321.html. Accessed 30 Sep 2022.
32. ISO 871:2022. Plastics—Determination of ignition temperature using a hot-air furnace. https://www.iso.org/standard/79709.html. Accessed 30 Sep 2022.
33. Carrasco F, Santana OO, Cailloux J, Sánchez-Soto M, Maspoch ML. Thermal degradation of poly (lactic acid) and acrylonitrile-butadiene-styrene bioblends: elucidation of reaction mechanisms. Thermochim Acta. 2017;654:157–67. https://doi.org/10.1016/j.tca.2017.05.013.
34. Ma H, Tong L, Xu Z, Fang Z, Jin Y, Lu F. A novel intumescent flame retardant: synthesis and application in ABS copolymer. Polym Degrad Stab. 2007;92(4):720–6. https://doi.org/10.1016/j.polymdegradstab.2006.12.009.
35. Ozkaraca AC, Kaynak C. Contribution of nanoclays to the performance of traditional flame retardants in ABS. Polym Compos. 2012;33(3):420–9. https://doi.org/10.1002/pc.22165.
36. Hong N, Zhan J, Wang X, Stec AA, Richard Hull T, Ge H, Xing W, Song L, Hu Y. Enhanced mechanical, thermal and flame retardant properties by combining graphene nanosheets and metal hydroxide nanorods for Acrylonitrile–Butadiene–Styrene copolymer composite. Compos Part A Appl Sci. 2014;64:203–10. https://doi.org/10.1016/j.compositesa.2014.04.015.

37. Yang Y, Kong W, Luo H, Cao X, Cai X. Enhancement of char-forming and water resistance on ABS modified by poly (4-nitrophenoxy)-phosphazene. J Appl Polym Sci. 2018;135(11):45988. https://doi.org/10.1002/app.v135.11.
38. Huang G, Han D, Jin Y, Song P, Yan Q, Gao C. Fabrication of nitrogen-doped graphene decorated with organophosphor and lanthanum toward high-performance ABS nanocomposites. ACS Appl Nano Mater. 2018;1(7):3204–13. https://doi.org/10.1021/acsanm.8b00411.
39. Stoliarov SI, Li J. Parameterization and validation of pyrolysis models for polymeric materials. Fire Technol. 2015;52(1):79–91. https://doi.org/10.1007/s10694-015-0490-1.
40. Dai PB, Wang DY, Wang YZ. Thermal degradation and combustion behavior of a modified intumescent flame-retardant ABS composite. J Thermoplast Compos Mater. 2009;23(4):473–86. https://doi.org/10.1177/0892705708103404.
41. Luo H, Zhou F, Yang Y, Cao X, Cai X. Gas–condensed phase flame-retardant mechanisms of tris(3-nitrophenyl) phosphine/triphenyl phosphate/ABS. J Therm Anal Calorim. 2017;132(1):263–73. https://doi.org/10.1007/s10973-017-6906-z.
42. Lu C, Chen T, Cai X. Halogen-free intumescent flame retardant for ABS/PA6/SMA alloys. J Polym Sci, Part B: Polym Phys. 2009;48(4):651–62. https://doi.org/10.1080/00222340903070342.
43. Hoang D, Kim J. Flame-retarding behaviors of novel spirocyclic organo-phosphorus compounds based on pentaerythritol. Macromol Res. 2015;23(7):579–91. https://doi.org/10.1007/s13233-015-3085-2.
44. Hu X, Guo Y, Chen L, Wang X, Li L, Wang Y. A novel polymeric intumescent flame retardant: synthesis, thermal degradation mechanism and application in ABS copolymer. Polym Degrad Stab. 2012;97(9):1772–8. https://doi.org/10.1016/j.polymdegradstab.2012.06.009.
45. Cao X, Yang Y, Luo H, Cai X. High efficiency intumescent flame retardancy between Hexakis (4-nitrophenoxy) cyclotriphosphazene and ammonium polyphosphate on ABS. Polym Degrad Stab. 2017;143:259–65. https://doi.org/10.1016/j.polymdegradstab.2017.07.022.
46. Jian RK, Chen L, Zhao B, Yan YW, Li XF, Wang YZ. Acrylonitrile–Butadiene–Styrene terpolymer with metal hypophosphites: flame retardance and mechanism research. Ind Eng Chem Res. 2014;53(6):2299–307. https://doi.org/10.1021/ie403726m.
47. Li J. A multiscale approach to parameterization of burning models for polymeric materials (Doctoral dissertation). Digital repository at the University of Maryland; 2014. https://doi.org/10.13016/M2XP4F. https://drum.lib.umd.edu/handle/1903/15897. Accessed 30 Sep 2022,
48. Hu D, Zhou Q, Zhou K. Combined effects of layered nanofillers and intumescent flame retardant on thermal and fire behavior of ABS resin. J Appl Polym Sci. 2019;136(46):48220. https://doi.org/10.1002/app.48220.
49. Yu CJ, Sunderland JE, Poli C. Thermal contact resistance in injection molding. Polym Eng Sci. 1990;30(24):1599–606. https://doi.org/10.1002/pen.760302408.
50. Yuan G, Li X, Yi J, Dong Z, Westwood A, Li B, Cui Z, Ye C, Zhang J, Li Y. Mesophase pitch-based graphite fiber-reinforced acrylonitrile butadiene styrene resin composites with high thermal conductivity. Carbon. 2015;95:1007–19. https://doi.org/10.1016/j.carbon.2015.09.019.
51. Trhlíková L, Zmeskal O, Psencik P, Florian P. Study of the thermal properties of filaments for 3D printing. AIP Confer Proc. 2016;1752(1):040027. https://doi.org/10.1063/1.4955258.
52. Fernandez AI, Martínez M, Segarra M, Martorell I, Cabeza LF. Selection of materials with potential in sensible thermal energy storage. Sol Energy Mater Sol Cells. 2010;94(10):1723–9. https://doi.org/10.1016/j.solmat.2010.05.035.
53. Bourell DL, Beaman JJ, Marcus HL, Barlow JW. Thermal properties of powders. In: 1990 international solid freeform fabrication symposium; 1990. https://repositories.lib.utexas.edu/handle/2152/64271. Accessed 30 Sep 2022.
54. Quill TJ, Smith MK, Zhou T, Baioumy MGS, Berenguer JP, Cola BA, Kalaitzidou K, Bougher TL. Thermal and mechanical properties of 3D printed boron nitride—ABS composites. Appl Compos Mater. 2017;25(5):1205–17. https://doi.org/10.1007/s10443-017-9661-1.
55. Wang S. Preparation and characterization of flame retardant ABS/montmorillonite nanocomposite. Appl Clay Sci. 2004;25(1–2):49–55. https://doi.org/10.1016/j.clay.2003.08.003.
56. Wu N, Li X. Flame retardancy and synergistic flame retardant mechanisms of acrylonitrile-butadiene-styrene composites based on aluminum hypophosphite. Polym Degrad Stab. 2014;105:265–76. https://doi.org/10.1016/j.polymdegradstab.2.
57. Liu B, Zhang Y, Wan C, Zhang Y, Li R, Liu G. Thermal stability, flame retardancy and rheological behavior of ABS filled with magnesium hydroxide sulfate hydrate whisker. Polym Bull. 2017;58(4):747–55. https://doi.org/10.1007/s00289-006-0695-z.
58. Shi L, Chew MYL. Fire behaviors of polymers under autoignition conditions in a cone calorimeter. Fire Saf J. 2013;61:243–53. https://doi.org/10.1016/j.firesaf.2013.09.021.
59. Schinazi G, Moraes d'Almeida JR, Pokorski JK, Schiraldi DA. Bio-based flame retardation of acrylonitrile–butadiene–styrene. ACS Appl Polym Mater. 2020;3(1):372–88. https://doi.org/10.1021/acsapm.0c01155.
60. Minea AA, Simionescu TM. The effect of montmorillonite clay and fire retardants on the heat of combustion of recycled acrylonitrile-butadiene styrene. Environ Eng Manag J. 2019;18(11):2387–96. https://doi.org/10.30638/eemj.2019.227.
61. Hermouet F, Rogaume T, Guillaume E, Richard F, Marquis D, Ponticq X. Experimental characterization of the reaction-to-fire of an Acrylonitrile-Butadiene-Styrene (ABS) material using controlled atmosphere cone calorimeter. Fire Saf J. 2021;121:103291. https://doi.org/10.1016/j.firesaf.2021.103291.
62. Simionescu TM, Minea AA, dos Reis PNB. Fire properties of acrylonitrile butadiene styrene enhanced with organic montmorillonite and exolit fire retardant. Appl Sci. 2019;9(24):5433. https://doi.org/10.3390/app9245433.
63. Realinho V, Arencón D, Antunes M, Velasco J. Effects of a phosphorus flame retardant system on the mechanical and fire behavior of microcellular ABS. Polymers. 2018;11(1):30. https://doi.org/10.3390/polym11010030.
64. Li J, Gong J, Stoliarov SI. Gasification experiments for pyrolysis model parameterization and validation. Int J Heat Mass Transf. 2014;77:738–44. https://doi.org/10.1016/j.ijheatmasstransfer.2014.06.003.
65. Hermouet F, Guillaume É, Rogaume T, Richard F, El Houssami M. Experimental determination of the evolution of the incident heat flux received by a combustible during a cone calorimeter test: Influence of the flame irradiance. J Fire Sci. 2021;39(2):119–41. https://doi.org/10.1177/0734904120970440.
66. Liang GL, Lin J, Dai PB, Lu YQ. Synergistic flame retardant effect of fumed silica and zinc borate with magnesium hydroxide in ABS based flame retardant composites. Appl Mech Mater. 2014;599–601:132–5. https://doi.org/10.4028/www.scientific.net/amm.599-601.132.
67. Wang Z, Yonggang L, Huijuan M, Wenpeng S, Tao L, Cuifen L, Zuxing C. Novel phosphorus-nitrogen-silicon copolymers with double-decker silsesquioxane in the main chain and their flame retardancy application in PC/ABS. Fire Mater. 2018;42(8):946–57. https://doi.org/10.1002/fam.2649.
68. Jian RK, Chen L, Chen SY, Long JW, Wang YZ. A novel flame-retardant acrylonitrile-butadiene-styrene system based

on aluminum isobutylphosphinate and red phosphorus: Flame retardance, thermal degradation and pyrolysis behavior. Polym Degrad Stab. 2014;109:184–93. https://doi.org/10.1016/j.polymdegradstab.2014.07.018.
69. Zhang W, Camino G, Yang R. Polymer/polyhedral oligomeric silsesquioxane (POSS) nanocomposites: an overview of fire retardance. Prog Polym Sci. 2017;67:77–125. https://doi.org/10.1016/j.progpolymsci.2016.09.011.
70. Hirschler MM. Poly(vinyl chloride) and its fire properties. Fire Mater. 2017;41(8):993–1006. https://doi.org/10.1002/fam.2431.
71. Carpenter K, Janssens M, Sauceda A. Using the cone calorimeter to predict FMVSS 302 performance of interior and exterior automotive materials. In: Society of automotive engineers world congress, Paper 2006-01-1270, Detroit, MI; 2006. https://doi.org/10.4271/2006-01-1270
72. Realinho V, Haurie L, Formosa J, Velasco JI. Flame retardancy effect of combined ammonium polyphosphate and aluminium diethyl phosphinate in acrylonitrile-butadiene-styrene. Polym Degrad Stab. 2018;155:208–19. https://doi.org/10.1016/j.polymdegradstab.2018.07.022.
73. Ghanbari D, Salavati-Niasari M, Esmaeili-Zare M, Jamshidi P, Akhtarianfar F. Hydrothermal synthesis of CuS nanostructures and their application on preparation of ABS-based nanocomposite. J Ind Eng Chem. 2014;20(5):3709–13. https://doi.org/10.1016/j.jiec.2013.12.070.
74. Hu XP, Guo YY, Xu QM, Heng HM, Li LJ. Synthesis of a novel intumescent flame retardant oligomer and its application in ABS copolymer. Adv Mater Res. 2011;391–392:204–8. https://doi.org/10.4028/www.scientific.net/AMR.391-392.204.
75. Nguyen C, Kim J. Synthesis of a novel nitrogen-phosphorus flame retardant based on phosphoramidate and its application to PC, PBT, EVA, and ABS. Macromol Res. 2018;16(7):620–5. https://doi.org/10.1007/bf03218570.
76. Xu S, Zhang L, Lin Y, Li R, Zhang F. Layered double hydroxides used as flame retardant for engineering plastic acrylonitrile–butadiene–styrene (ABS). J Phys Chem Solids. 2012;73(12):1514–7. https://doi.org/10.1016/j.jpcs.2012.04.011.
77. Jang J, Kim J, Bae JY. Synergistic effect of ferric chloride and silicon mixtures on the thermal stabilization enhancement of ABS. Polym Degrad Stab. 2015;90(3):508–14. https://doi.org/10.1016/j.polymdegradstab.2005.04.014.
78. Wang J, Wu S. On the flammability of the electron-beam-induced grafting of ABS and SBS copolymers, studied by LOI/CONE/XPS. J Fire Sci. 2001;19(2):157–72. https://doi.org/10.1106/QTTB-0UVJ-8U5D-V5X9.
79. Balart R, Garcia-Sanoguera D, Quiles-Carrillo L, Montanes N, Torres-Giner S. Kinetic analysis of the thermal degradation of recycled acrylonitrile-butadiene-styrene by non-isothermal thermogravimetry. Polymers. 2019;11(2):281. https://doi.org/10.3390/polym11020281.
80. Suzuki M, Wilkie CA. The thermal degradation of acrylonitrile-butadiene-styrene terpolymer as studied by TGA/FTIR. Polym Degrad Stab. 1995;47(2):217–21. https://doi.org/10.1016/0141-3910(94)00122-o.
81. Babrauskas V. Chapter 26: heat release rates. SFPE handbook of fire protection engineering. New York: Springer; 2016: pp. 799–904. https://doi.org/10.1007/978-1-4939-2565-0_26
82. Lautenberger C, Rein G, Fernandez-Pello C. The application of a genetic algorithm to estimate material properties for fire modeling from bench-scale fire test data. Fire Saf J. 2006;41(3):204–14. https://doi.org/10.1016/j.firesaf.2005.12.004.